Journal of Physics:
Conference Series

PAPER • OPEN ACCESS

Enhancing Surface Hydrophobicity of AISI 304 Stainless Steel via Laser Texturing

To cite this article: M. Isa Rahim *et al* 2025 *J. Phys.: Conf. Ser.* **2933** 012006

Enhancing Surface Hydrophobicity of AISI 304 Stainless Steel via Laser Texturing

M. Isa Rahim[1], S.N. Aqida[1,2*], M.S. Salwani[1], S. Ahmad Syarizan[1]

[1]Faculty of Mechanical and Automotive Engineering Technology, Universiti Malaysia Pahang Al-Sultan Abdullah, 26600 Pekan, Pahang, Malaysia
[2]Automotive Engineering Centre, Universiti Malaysia Pahang Al-Sultan Abdullah, 26600 Pekan, Pahang, Malaysia

*E-mail: aqida@umpsa.edu.my

Abstract. The wettability performance of 304 stainless steel surfaces that were treated by multipulse laser processing under different parameters is studied in this paper. For modifying the surface of stainless steel, we used an x-y computer numerical control (CNC) fibre laser system with a 1064 nm wavelength. The hydrophobicity of all surfaces was evaluated through water contact angles (WCA) at different translational speeds (20–150 mm/s) and laser powers (4–20 W). Results show a spectrum of surface wettability ranging from hydrophilic (WCA<90°) to hydrophobic properties (90<WCA<150°). Hydrophobic surfaces were mainly associated with the samples processed at higher speeds and power settings while hydrophilic results were observed due to lower speeds and power settings. The highest hydrophobicity of WCA = 142.05° was obtained at a speed of 20 mm/s and laser power of 8 W. Meanwhile, the highest degree of hydrophilicity was observed at a speed of 20 mm/s and the lowest power level of 4 W, which possessed a WCA of 62.49°. Therefore, this study highlights the importance of laser parameters in the surface wettability modification process. These results are significant to applications requiring specific surface characteristics, such as anti-slip, anti-fog and self-cleaning. The findings provide a comprehensive review of the application of laser processing in preparing surface treatment with suitable properties for various industrial and biomedical applications.

Keywords: Stainless steel, laser texturing, wettability, fibre laser, hydrophobic surface

1. Introduction

The alteration of surface wettability is an essential component of material science, carrying substantial implications for industrial and biomedical applications [1]. Stainless steel is widely recognized for its durability, resistance to corrosion, and mechanical strength, making it a material of choice in numerous industries. However, the surface properties can be further optimized to satisfy specific functional requirements, including hydrophobicity. The properties outlined are essential for applications that require anti-slip surfaces, anti-fogging features, and self-cleaning mechanisms [3][4].

Laser processing has developed into a flexible and accurate method for surface modification, allowing for the customization of material properties at micro and nano scales [5]. Adjusting laser parameters, including speed and power, allows for the manipulation of the contact angle of surfaces, thus enabling control over their wettability. Prior studies have shown that laser-induced surface structures can markedly modify the hydrophilic and hydrophobic characteristics of materials, providing a means for tailored surface functionalities [6][7].

This study investigates the wettability characteristics of stainless steel surfaces exposed to different laser processing parameters. Systematic experimentation was conducted using various laser speeds ranging from 20 to 150 mm/s and power settings between 4 and 20 watts. The contact angles (WCA) were measured with precision to categorize the surfaces as either hydrophilic or hydrophobic. The findings indicate a range of wettability behaviours, highlighting the influence of laser parameters on surface properties. This analysis enhances the understanding of laser-material interactions and provides insights for optimizing surface properties for various applications [8].

2. Experimental Work

A fibre laser system operating in continuous mode at a wavelength of 1064 nm was utilized for surface texturing during the resurfacing process. The laser texturing procedure was controlled using LightBurn software, and the experimental setup is illustrated in Figure 1.

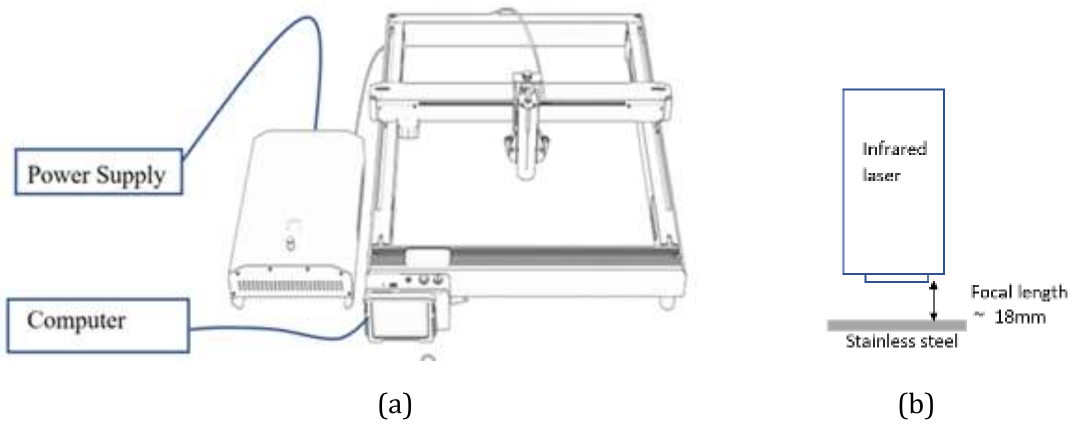

Figure 1. Schematic diagram of the experimental setup for (a) laser texturing of stainless steel sheets, and (b) focal length measurement

In this study, 304 stainless steel with a thickness of 1.0 mm and dimensions of 5x5 mm^2 was used as the substrate material. The chemical composition of the material is provided in Table 1. Laser texturing was performed with varying independent variables, specifically scanning speed and power. A two-level factorial design of experiments was employed, with five levels of scanning speed and laser power. The laser texturing parameters are detailed in Table 2.

The independent variables were scanning speed, laser power, and the maximum and minimum settings of the laser process, aimed at determining their impact on laser parameter performance for contact angle measurements using this study. Table 2 outlines the two factors and five levels of laser parameters. The data analysis of variance (ANOVA) was conducted to

Journal of Physics: Conference Series **2933** (2025) 012006 doi:10.1088/1742-6596/2933/1/012006

evaluate the effect of laser process parameters on surface integrity outcomes. The results from multiple regression analysis of the ANOVA were used to develop an empirical model.

Table 1. Chemical compositions of AISI 304 stainless steel

Element	**C**	**Cr**	**Ni**	**Mn**	**Si**	**P**	**S**	**Fe**
Content wt%	0.07	15.56	8.5	1.25	0.502	0.07	0.003	Bal

Table 2. Laser parameters for stainless steel surface wettability modification with two factors and five levels.

Factors	Scanning Speed (mm/s)	Laser Power (W)
Minimum	20	4
Maximum	150	20

The water contact angle (WCA) of the modified stainless steel surface was measured using a sessile drop method. Type II reagent water, conforming to ASTM D1193 specifications, was used as the test liquid. The CA measurements were conducted following ASTM D7334 guidelines [9], utilizing a Hamilton microliter syringe to dispense a 4 μL droplet onto the stainless steel surface. Measurements were taken within 30 seconds to minimize angle changes due to evaporation [9]. A microscope, in accordance with ASTM D5725 [10], with a maximum magnification of 100×, was connected to a laptop to capture images of the droplet. The images underwent conversion to grayscale and were processed utilizing ImageJ software. Additional contact angle analysis was conducted through the Low Bond Axisymmetric Drop Shape Analysis (LB-ADSA) plugin. Figure 2 illustrates the schematic setup of the sessile drop test.

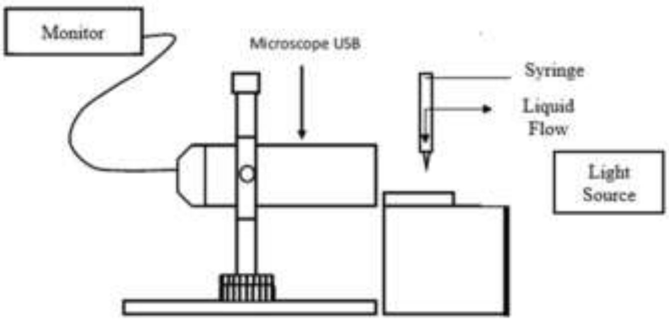

Figure 2. A schematic setup of the sessile drop test [11]

3. Results and Discussion

Table 3 presents the contact angles measured through laser processing. The findings demonstrate considerable variation in contact angles as influenced by the laser processing parameters, with measurements spanning from 62.49° to 142.05°. The minimum contact angle recorded was 62.49°, attained at a laser speed of 20 mm/s and a laser power setting of 4 W, signifying a hydrophilic surface. The maximum contact angle recorded was 142.05°, attained at a

Journal of Physics: Conference Series **2933** (2025) 012006 doi:10.1088/1742-6596/2933/1/012006

laser speed of 20 mm/s and a power setting of 8 W. This measurement suggests a hydrophobic surface nearing superhydrophobicity, which is defined as exceeding 150°. The results indicate a significant impact of laser speed and power on the wettability properties of stainless steel surfaces. This emphasizes the need for additional research to optimize laser parameters for achieving the desired surface characteristics. The results indicate a significant enhancement in contact angle values, with the peak recorded at a speed of 20 mm/s and a power setting of 8 W during run 24, achieving a measurement of 142.05°, as detailed in Table 3.

Table 3. Results of contact angles for samples based on laser texturing speed and laser power

Run	Scanning speed (mm/s)	Laser power (W)	Contact angle (°)	
1	150	20	100.543	
2	118	20	140.038	
3	118	16	94.885	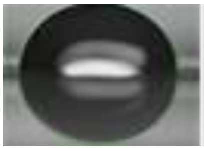
4	85	16	127.709	
5	53	16	105.136	
6	85	20	91.383	
7	85	12	123.178	
8	53	20	68.061	

Journal of Physics: Conference Series **2933** (2025) 012006 doi:10.1088/1742-6596/2933/1/012006

Cont. Table 3

Run	Scanning speed (mm/s)	Laser power (W)	Contact angle (°)	
9	20	20	78.035	
10	150	20	94.885	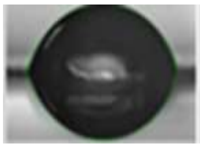
11	150	16	128.176	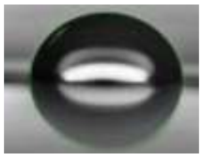
12	20	16	81.798	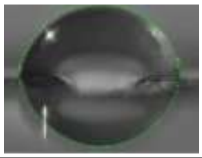
13	150	12	73.995	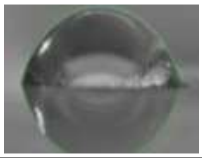
14	85	12	118.553	
15	118	12	123.178	
16	53	12	99.526	
17	20	12	92.765	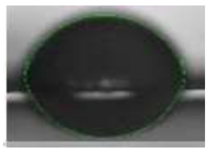
18	20	8	73.317	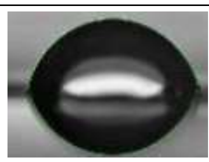

Journal of Physics: Conference Series **2933** (2025) 012006 doi:10.1088/1742-6596/2933/1/012006

Cont. Table 3

Run	Scanning speed (mm/s)	Laser power (W)	Contact angle (°)	
19	53	8	103.505	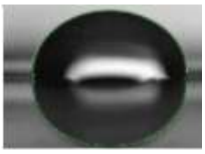
20	85	8	121.546	
21	118	8	100.376	
22	150	8	77.018	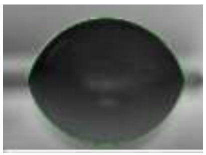
23	20	4	62.49	
24	20	8	142.054	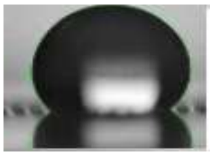
25	53	4	82.75	
26	85	4	81.058	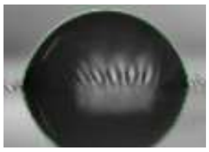
27	118	4	83.909	
28	150	4	69.892	

3.1 Water Contact Angle (WCA)
Laser-textured 304 stainless steel surfaces demonstrate different water contact angles (WCAs) influenced by the laser scanning speed and power settings utilized. The resulting WCAs are summarized in Table 3. The untreated 304 stainless steel surface was initially hydrophilic, with a WCA of 49.13°. After laser texturing with different parameters—specifically, at respective scanning speeds and powers of 20 mm/s, 4 W power, and 150 mm/s,16 W power, the WCA increased to 62.49°and 128.18°. Overall, the WCA increased after laser surface texturing, indicating a reduction in hydrophilicity and a shift toward hydrophobicity. The scanning speed and power significantly influence the CA, highlighting their importance in optimizing laser processing parameters.

3.2 ANOVA Result
The mathematical model of the responses, specifically the contact angle, was analyzed and validated through the application of analysis of variance (ANOVA). The data collected from the experimental runs underwent analysis. ANOVA comprises a series of statistical models utilized to analyze and determine the most significant factors influencing the contact angle. This study employed ANOVA at a 5% significance level, utilizing a p-value threshold of less than 0.00500 to analyze and identify the impact of significant laser parameters on the evaluation of laser processing performance, including contact angle. The primary effects and interaction effects were illustrated based on the results of the ANOVA analysis. The contact angle response exhibited a range from 62.460 to 142.0540, resulting in a ratio of maximum to minimum response of 2.27. The primary effects to be examined include the sum of squares, degrees of freedom (DF), mean square, F value, residual, and total of mean corrected (Cor Total). Table 4 presents the analysis of variance (ANOVA) for the response contact angle in laser processing, following transformation through Response Surface Methodology (RSM) analysis utilizing historical data, as processed by the Design Expert software. The model F-value of 3.59 indicates that the model demonstrates statistical significance.

Table 4. ANOVA for Quadratic Model Result for Contact Angle on Laser Processing

Source	Sum of Square	DF	Mean Square	F-Value	P-Value	
Model	6426.8	5	1285.36	3.59	0.016	significant
A-Speed	311.49	1	311.49	0.8689	0.3614	
B-Power	748.81	1	748.81	2.09	0.1625	
AB	1407.48	1	1407.48	3.93	0.0602	
A^2	2144.18	1	2144.18	5.98	0.0229	
B^2	2083.09	1	2083.09	5.81	0.0247	
Residual	7886.71	22	358.49			
Cor Total	14313.51	27				

The F-value obtained from the mean square was transformed into its associated P-value. The ANOVA analysis indicated a low probability value, with Prob>F approximately 3.59% (P = 0.0359). Furthermore, when the P-value is less than 0.0500, the relationship between the factors (A-Speed, B-Power, and their interactions) and the response is considered statistically significant.

Factors with 'Prob > F' values less than 0.0500 indicate that the model terms are statistically significant [12]. The final statistical equation model was developed using ANOVA, reflecting the actual factors, and is presented as follows in Equation (1):

$$\text{Contact angle} = +45.18302 + 0.582025 \times \text{Speed} + 6.43752 \times \text{Power} + 0.026793 \times \text{Speed} \times \text{Power} - 0.004891 \times \text{Speed}^2 - 0.324275 \times \text{Power}^2 \quad (1)$$

This final statistical model used scanning speed and power as its inputs. The predictions made by the model were generally accurate, with an average error of less than 10% when compared to experimental results. The model's goodness of fit was quantified using R-squared and adjusted R-squared values, which were recorded at 44.90% and 32.38%, respectively.

Figures 3(a) and 3(b) provide graphical representations of the response surface in 3D and its corresponding contour plot, respectively. The analysis of the 3D response surface plot 3(a) demonstrates a significant nonlinear relationship between the contact angle and the parameters of laser power (B) and speed (A). The water contact angle ranges from approximately 40° to 160°, indicating high sensitivity to changes in laser power and speed. At lower power levels (8 W to 12 W), increasing speed results in a moderate increase in the contact angle, while at higher power levels (16 W to 20 W), the effect of increasing speed is more pronounced. There is also a clear interaction effect where the contact angle peaks at moderate speed values (72 to 98 mm/s) and high power (16 W to 20 W). This suggests that an optimal combination of speed and power is crucial to achieve maximum contact angle. Contour plot 3(b) illustrates that the contact angle exhibits increases with rising speed and power, reaching a maximum within a specific central region. This central region, characterized by the highest contour level (110°), indicates the optimal combination of speed and power for achieving the maximum contact angle. Outside this central region, the contact angle decreases as either speed or power deviates from these optimal values.

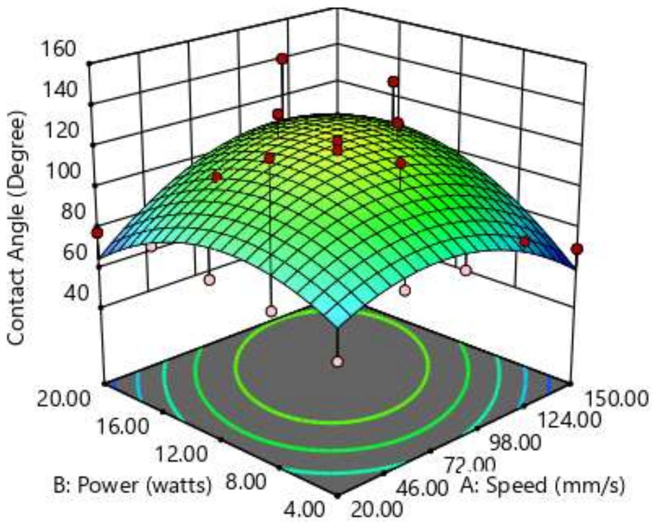

Figure 3. (a) A three-dimensional response surface graph demonstrating the effect of two laser parameters (scanning speed, power) on the contact angle

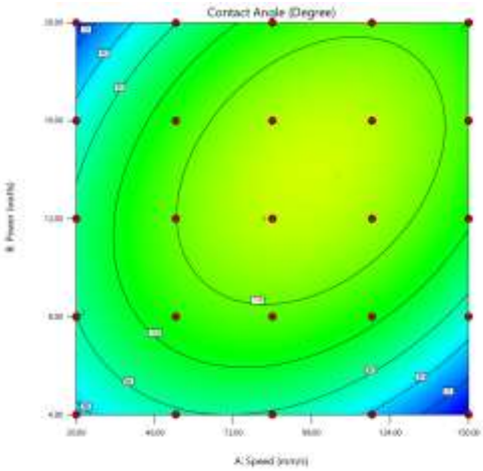

Figure 3. (b) Contour plot depicting the effects of scanning speed and laser power on water contact angle.

Figure 4 (a) presents the normal probability plot of residuals for water contact angle, generated using Design Expert software. The plot illustrates that the surface roughness values largely align along a straight line, indicating a normal distribution. The data distribution is satisfactory, as all points are well-aligned. Figure 4(b) illustrates the comparison between predicted and actual response plots, which is essential for detecting outliers identified by the model. The model exhibits a close alignment with the observed values, indicating a strong correlation between the predicted contact angle values generated by the model and the actual experimental data.

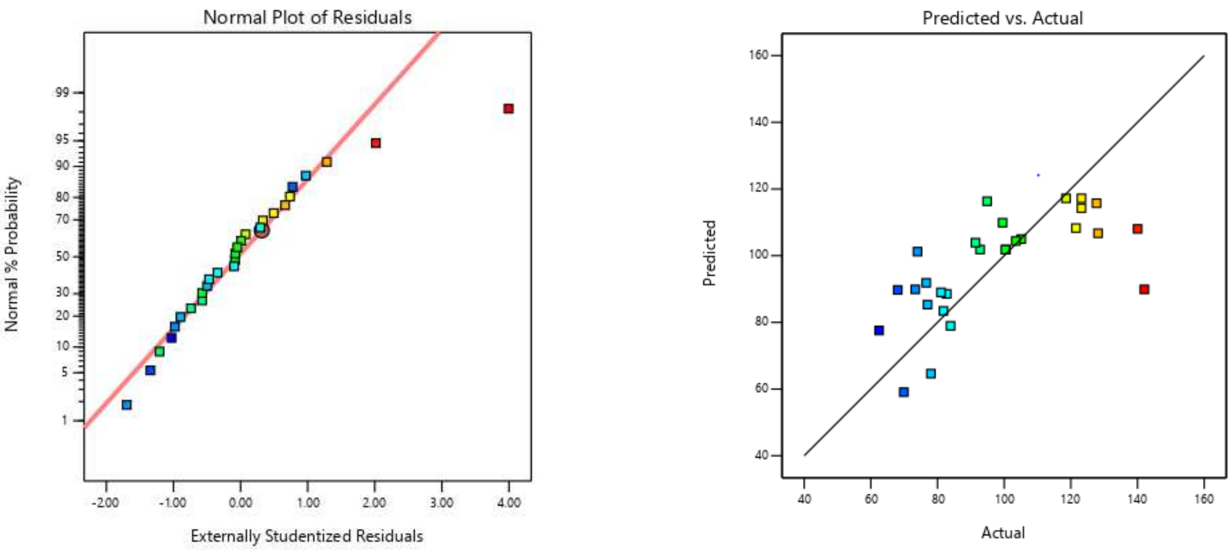

(a) (b)

Figure 4. The normal probability plot of residuals for the contact angle is depicted in Figure 4(a), illustrating the distribution of residuals. Figure 4(b) presents the graph of predicted versus actual contact angle values, showcasing the relationship between the experimental results and the model's predictions.

3.3 Morphology Analysis

AISI 304 surface morphology was studied by using SEM-EDX (Figure 5(a-f)) under different laser processing parameters and TR200 Roughness Tester values were measured to determine the surface roughness. Abstract Laser texturing was used to obtain different levels of roughness on the surface morphology of an AISI 304 stainless steel. The hydrophobicity of the sample is further enhanced by micro- and nano-gaps. Figure (5a) scanning speed =150 mm/s, laser power =100 W shows the air pockets limit contact-opportunity to the water surface with a high water contact angle of 100.54°. This is indicative of the contribution of roughness to reduced wettability, which enhances the hydrophobic effect.

In addition, the chemical composition, in particular, high oxygen content indicates oxides that change surface energy and consequently promote hydrophobicity. Fe, Cr, and Ni also will combine to form an alloying element that forms a passivation layer that is stable on the surface upon flashing inside contact with water. The synergistic effect between the high Ra of 6.638 μm and metal oxide composition provides a surface that can efficiently prevent water adhesion.

In Figure 5(b), the scanning speed of 118 mm/s and laser power of 100 W, shows the sample imparting hydrophobic properties due to the combined effect of gross morphology and chemistry combination. Rough (Ra of 6.503 μm) and textured surfaces decrease water adhesion by a phenomenon known as the air pocket effect; the rough surface pattern creates micro- and nano-scale pockets of air that limit interactions between the water molecules and solid surface. The high oxygen content indicates iron oxide, which further increases the hydrophobicity through its presence (16.37 wt%) lowering the surface energy at the same time.

Figure 5(c) of 85 mm/s scanning speed and 80 W laser power shows the aforementioned surface morphology features are well consistent with the high value of 5.711 μm for Ra which can be seen in SEM images as a granular and irregular roughness pattern. This roughness further helps the material to hold up air pockets beneath water droplets due to the Cassie-Baxter model [13] which parallelly causes hydrophobicity that can be seen in water contact angle high value (127.709°). The relation between the surface structure and its roughness is crucial to understanding its wetting properties.

Moreover, from the point of view of elemental composition, chromium and iron dominate which implies oxide formation at the surface modifying the surface energy [14]. Together with high roughness, these oxides enhance the hydrophobic properties of this material.

Figure 5(d) shows a rough and textured surface morphology with ridges and irregularities which through SEM-EDX analysis, contribute to the measured surface roughness value of 5.577 μm. This high surface roughness is seen to affect the wetting behaviour of the material, as evidenced by the water contact angle of 118.55°, which shows moderate hydrophobicity. According to the Cassie-Baxter model, a rough surface helps trap air pockets under water droplets, reducing surface wettability and increasing hydrophobicity.

At a scanning speed of 20 mm/s and laser power of 40 W, a rough and textured surface morphology with varying ridges, associated with a high roughness value (Ra = 5.641 μm). This roughness causes a significant increase in hydrophobicity, resulting in a high water contact angle of 142.05° and approaching superhydrophobicity (WCA>150°). EDX analysis identified a material composition of mainly iron (62.45 wt%) with significant amounts of chromium (25.24 wt%) and nickel (12.31 wt%), typical of stainless steel. The combination of topological surface roughness and chemical composition, including chromium and nickel, is proven to reduce surface energy and increase water repellency.

Figure 5(f) shows a smooth rough surface with parallel stripes, corresponding to the indicated low roughness value (Ra = 0.780 μm) and a hydrophilic water contact angle of 62.49°. From the EDX Analysis, the material composition is mainly iron (75.92 wt%) with significant chromium (20.73 wt%) and little oxygen (2.22 wt%), This shows the composition of stainless steel with minimal oxidation. The smooth morphology and high chromium content can reduce water trapping and surface energy, resulting in increased.

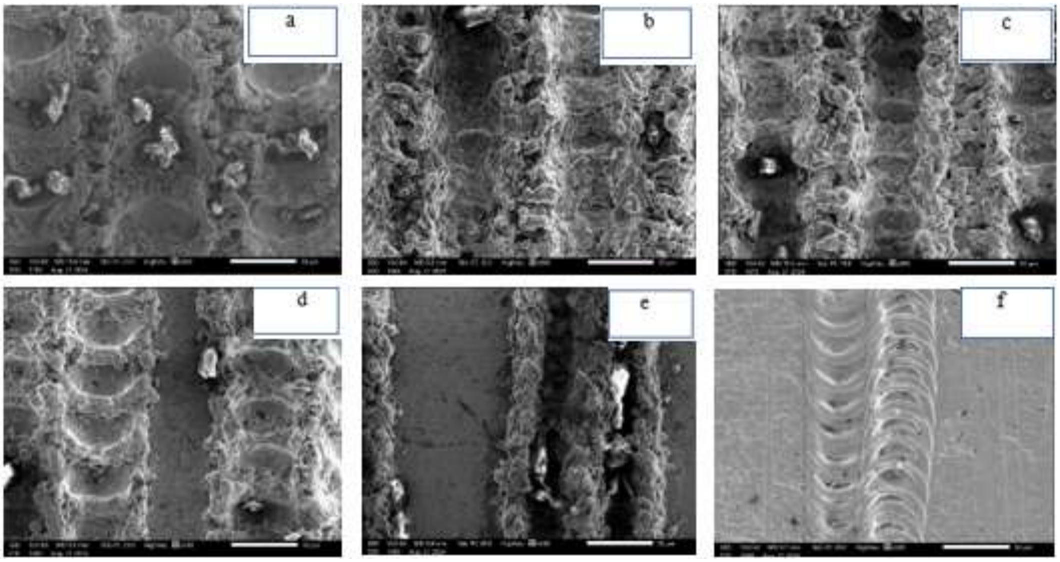

Figure 5. SEM Images of laser-textured 304 stainless steel surfaces under varying laser processing parameter

4. Conclusions

The results show that the processing parameters of lasers exert a significant influence on the surface wettability conversion from hydrophilicity to hydrophobicity of stainless steel. Depending on the laser speed and power, water contact angles (WCA) can be controlled in the range of hydrophilic (WCA>90°) to hydrophobic state (WCA>150°). Hydrophobic properties with a water contact angle of up to 142.05° were achieved from the low-speed (20 mm/s) and moderate-power (8 W) surface processing. Conversely, the surface treated samples at low power (4 W) resulted in less hydrophobicity since a WCA as low as 62.49° was produced. The results presented in this research reinforced the nature of controlling laser parameters to attain optimum properties, which have major implications for a wide range of applications needing tailored surface characteristics.

5. Acknowledgements

The authors would like to express their gratitude and thanks to Universiti Malaysia Pahang Al-Sultan Abdullah for laboratory facilities and funding under RDU230398 UMPSA Fundamental Research Grant.

Journal of Physics: Conference Series **2933** (2025) 012006 doi:10.1088/1742-6596/2933/1/012006

References

[1] B. Bhushan, "Biomimetics: Lessons from Nature – An Overview," Philosophical Transactions of the Royal Society: Mathematical, Physical and Engineering Sciences, vol. 367, no. 1893, pp. 1445-1486, 2009
[2] J. R A. Davis, Stainless Steels. ASM International, 1994.
[3] C. Neinhuis and W. Barthlott, "Characterization and Distribution of Water-repellent, Self-cleaning Plant Surfaces," Annals of Botany, vol. 79, no. 6, pp. 667-677, 1997.
[4] J. Yong et al., "Femtosecond Laser Weaving Superhydrophobic Patterns with Hierarchical Structures on Flexible PET Substrates," Applied Surface Science, vol. 399, pp. 580-586, 2017
[5] D. Bäuerle, Laser Processing and Chemistry. Springer, 2013.
[6] A. Y. Vorobyev and C. Guo, "Enhanced Absorptance of Gold Following Multipulse Femtosecond Laser Ablation," Physical Review B, vol. 80, no. 11, p. 115421, 2009
[7] V. Zorba, E. Stratakis, M. Barberoglou, C. Fotakis, and E. Spanakis, "Laser Micro/nano Textured Biomimetic Surfaces with Controlled Wetting and Optical Properties," Acta Biomaterialia, vol. 4, no. 5, pp. 1825-1832, 2008.
[8] Y. Wu, F. Zhang, Y. Zhang, and L. Liu, "Surface Wettability Modification of Stainless Steel via Laser Processing and Its Application," Materials, vol. 14, no. 12, p. 3340, 2021
[9] ASTM D7490, "Measurement of the surface tension of solid coatings, substrates, and pigments using contact angle measurements (ASTM Standard D7490-13)," ASTM International, pp. 1-5, 2013. doi: 10.1520/D7490-13.
[10] R. Coatings, "Standard practice for surface wettability of coatings, substrates, and pigments by advancing contact angle measurement (ASTM Standard D7334-08R13)," Annual Book of ASTM Standards, vol. i, no. C, pp. 8-10, 2011. doi: 10.1520/D7334-08R13.
[11] K. N. Najwa, M. Hilmi, S. N. Aqida, and I. Ismail, "Hydrophobicity of laser-textured soda-lime glass," in Journal of Physics: Conference Series, vol. 2688, no. 1, p. 012021, 2024, IOP Publishing.
[12] D. C. Montgomery, Design and Analysis of Experiments, 9th ed., John Wiley & Sons, 2017.
[13] A. B. D. Cassie and S. Baxter, "Wettability of porous surfaces," *Trans. Faraday Soc.*, vol. 40, pp. 546–551, 1944. doi: 10.1039/TF9444000546.
[14] J. M. White and D. J. Dwyer, "Oxides on Metal Surfaces: Effects on Surface Energy and Wettability," *Surface Science Reports*, vol. 12, no. 3, pp. 155–230, 1991. doi: 10.1016/0167-5729(91)90001-J.
[15] A. Ramli, R. I. Raja Abdullah, M. H. Abu Bakar, M. S. Kasim, M. A. A. Rahman, and M. A. Mohd Zakaria, "Investigation on improvement of surface roughness using rotary ultrasonic assisted machining technique for hardened steel material," *J. Mech. Eng.* (JMechE), no. 1, pp. 118-134, 2017.